SPATIAL AND ENERGY DISTRIBUTIONS OF SATELLITE-SPEED HELIUM ATOMS REFLECTED FROM SATELLITE-TYPE SURFACES*

S. M. Liu, W. E. Rodgers, and E. L. Knuth
Chemical, Nuclear, and Thermal Engineering Department
UCLA
Los Angeles, CA 90024

Interactions of satellite-speed helium atoms (accelerated in an expansion from an arc-heated supersonic-molecular-beam source) with practical satellite surfaces have been investigated experimentally. The molecular-beam system is that described by Hays et al. [1] and by Liu [2]; the arc-heated source is the one developed by Young [3]. The beam was characterized by a multi-disk velocity selector similar to that described by Trujillo et al. [4]. The density and energy distributions of the scattered atoms were measured using a detection system developed for this study. This detection system includes (a) a target positioning mechanism, (b) a detector rotating mechanism, and (c) a mass spectrometer and/or a retarding-field energy analyzer.

Since the background gas of the beam species also contributed to the measured spectrum, it was necessary to subtract this contribution in order to obtain the reflected-beam energy distributions. This subtraction was facilitated by measuring two spectra (one for the reflected beam plus background and one for the background alone) under the same operating conditions. Both the background spectrum and the reflected-beam spectrum were least-square fitted using a high-order Chebyshev polynomial function. The differential energy distributions f(E) were obtained by simple differentiation of the fitted functions. The mean reflected-beam energy at a given scattering position (cf. Fig. 1) was evaluated from

$$E_r(\theta_i,\theta_r,\phi) = \tilde{E}_r - \tilde{E}_{ref} + 0.05 \text{ (eV)} \tag{1}$$

where

$$\tilde{E}(\theta_i,\theta_r,\phi) = \int f(E)\cdot E\cdot dE / \int f(E)\cdot dE \tag{2}$$

and 0.05 eV is the thermal energy of the background gas at 296°K. The differential energy accommodation coefficient at a given scattering position was obtained using

$$[A.C.]_E(\theta_i,\theta_r,\phi) = \frac{E_i - E_r(\theta_i,\theta_r,\phi)}{E_i} \tag{3}$$

where E_i is the incident-beam energy. The overall energy accommodation for a given incidence angle was evaluated then using

$$[A.C.]_E(\theta_i) = \sum_{\theta_r} \sum_{\phi} n_i(\theta_i,\theta_r,\phi)\ [A.C.]_E(\theta_i,\theta_r,\phi) \tag{4}$$

where $n_i(\theta_i,\theta_r,\phi)$ is the normalized spatial density-distribution function of reflected helium atoms.

Spatial distributions of satellite-speed helium beams scattered from cleaned 6061-T6 aluminum plate, anodized aluminum foil, white paint and quartz surfaces

*Supported by NASA under Grant No. NGR 05-007-416.

were measured. Both in-plane (i.e., in the plane containing the incident beam and the surface normal) and out-of-plane spatial distributions of reflected helium atoms were measured for six different incidence angles (0°, 15°, 30°, 45°, 60°, and 75° from the surface normal). A typical spatial scattering distribution is shown in Fig. 2. The center of the polar diagram corresponds to the point of impingement. The incident beam impinges on the test surface (which coincides with the surface of the page) from the bottom of the diagram with the given incidence angle measured from the surface normal. The dashed lines at constant value of θ_r indicate detector paths (i.e., from $\phi = 0°$ to $\phi = 90°$). The most interesting feature of these scattering patterns is the prominent backscattering of the incident helium atoms (i.e., a large fraction of the incident atoms are scattered back in the vicinity of the incident beam), particularly as the incidence angle increases toward the surface tangent (i.e., for large values of θ_i). This large fraction of backscattering could be due to the gross surface roughness and/or the relative lattice softness of the aluminum satellite surfaces, and could yield drag coefficients which are higher than for surfaces with either forward-lobed or diffusive (cosine) scattering patterns.

Energy distributions of satellite-speed helium atoms scattered from a cleaned 6061-T6 aluminum satellite surface were measured for six different incidence angles (θ_i = 0°, 15°, 30°, 45°, 60°, and 75° from the surface normal). For each incidence angle, distributions were measured at approximately sixty scattering positions. Typical results are given in Table 1. This table also includes standard deviations (σ) of the reflected-beam energy-spectrum data from the least-square fitted curves and the normalized spatial-distribution function of the reflected helium atoms obtained from the measured spatial distributions shown in Fig. 2. The measured differential accommodations obtained show some fluctuations, due perhaps to the weak signal-to-noise ratio which results from the relatively diffusive scattering from the satellite-type aluminum surface. The results also indicate a weak dependence of accommodation on scattering angle, i.e., the $(A.C.)_E(\theta_i,\theta_r,\phi)$ decreases as the scattering direction shifts toward the surface tangent.

The overall energy accommodation coefficient for a beam with a given incidence angle was evaluated then using Eq. (4) and data such as given in Table 1. The results are shown in Fig. 4. It is seen that the mean accommodation coefficient varies between 50% and 65%, and is slightly higher for a glancing beam than for a normal-incidence beam.

Similar measurements are being made for anodized aluminum surfaces. The data analysis is being extended to include drag coefficients.

References

1. W. J. Hays, W. E. Rodgers, and E. L. Knuth, "Scattering of Argon Beams with Incident Energies up to 20 eV from a (111) Silver Surface," J. Chem. Phys. 56:1652-1657, 15 Feb. 1972.
2. S. M. Liu, "An Experimental Study of Interactions of Hyperthermal Atomic Beams with (111) Silver Surfaces and Adsorbed Molecules," UCLA-ENG-7510. Los Angeles: UCLA School of Engineering and Applied Science, Feb. 1975.
3. W. S. Young, W. E. Rodgers, and E. L. Knuth, "An Arc Heater for Supersonic Molecular Beams," Rev. Sci. Instrum. 40:1346-1347, October 1969.
4. S. M. Trujillo, P. K. Rol, and E. W. Rothe, "Slotted-Disk Velocity Selector of Extended Range," Rev. Sci. Instrum. 33:841-843, August 1962.

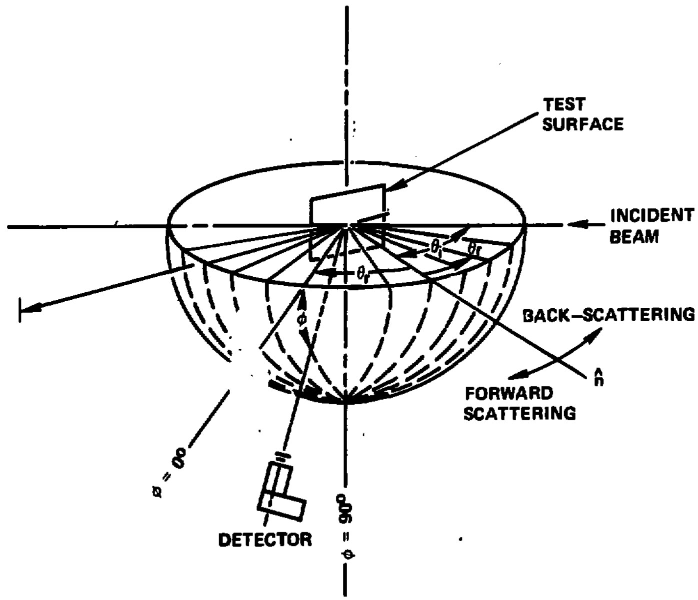

Figure 1. Schematic Diagram of the Scattering System.

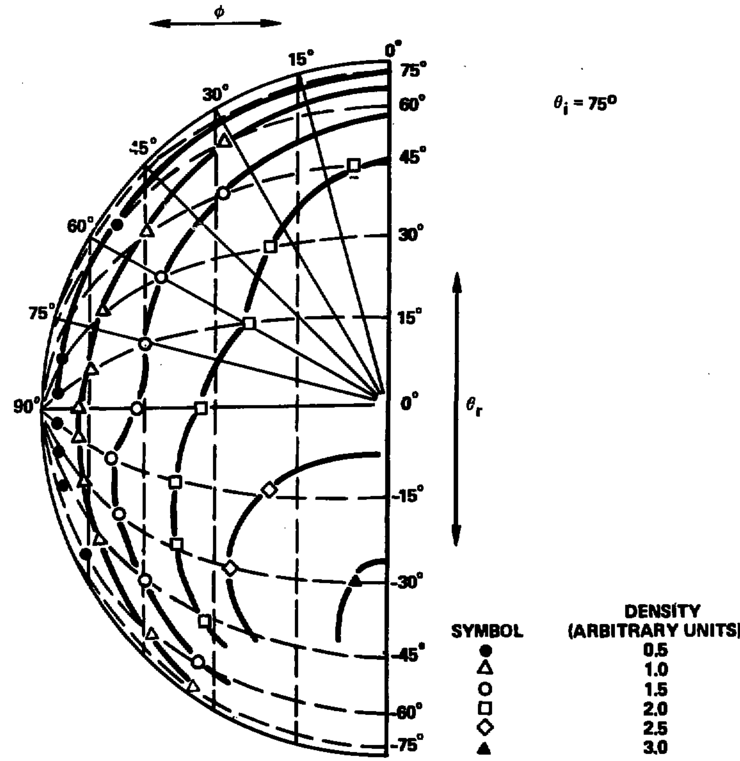

Figure 2. Polar Plot of Scattered-Beam Density Distribution for 7000 m/sec Helium Beam Scattered from Cleaned 6061-T6 Aluminum Plate at 75° Incidence Angle.

Table 1.

The Differential Energy Accommodation Coefficients and the Normalized Spatial Density Distribution for 7000 m/sec Helium Beam Scattered from Cleaned 6061-T6 Aluminum Plate at 75° Incidence Angle.

ϕ \ θ_r	-75°	-60°	-45°	-30°	-15°	±0°	15°	30°	45°	60°	75°
0°				72 7.0 11	66 6.1 8	64 5.4 13	51 5.0 20	50 4.8 16	45 4.5 30	–	–
15°				63 6.1 11	70 5.8 13	63 5.2 13	59 4.9 20	59 4.5 21	–	–	–
30°				80 5.4 13	60 5.0 13	53 4.5 14	–	–	–	–	–
45°	79[a] 1.9[b] 17	79 2.2 20	84 3.4 18	78 3.9 16	58 4.0 15	–	–	–	–	–	–
60°	66[c] 1.1 23	78 1.8 20	73 2.2 16	75 2.5 16	52 2.5 17	–	–	–	–	–	–
75°	–	–	–	–	–	–	–	–	–	–	–

NOTE:

(a) The Differential Accommodation Coefficient (%)
(b) The Normalized Spatial Density (%)
(c) Standard Deviation (%)

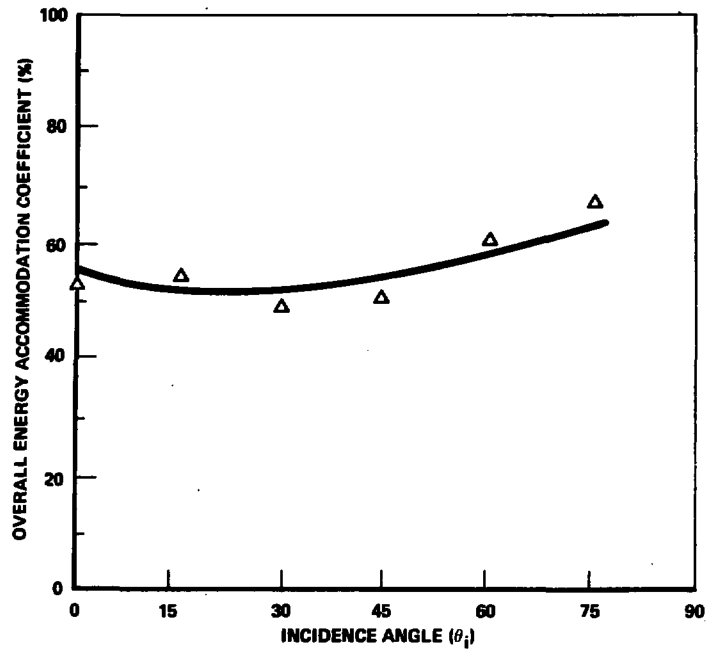

Figure 3.

Overall Energy Accommodation Coefficient of a Satellite-Speed Helium Beam (1.02 eV) Scattered From a Cleaned 6061-T6 Aluminum Surface as a Function of the Incidence Angle.